Stem Cell Reports
Report
OPEN ACCESS

CPM Is a Useful Cell Surface Marker to Isolate Expandable Bi-Potential Liver Progenitor Cells Derived from Human iPS Cells

Taketomo Kido,[1,*] Yuta Koui,[1] Kaori Suzuki,[1,2] Ayaka Kobayashi,[1] Yasushi Miura,[1] Edward Y. Chern,[1,3] Minoru Tanaka,[1] and Atsushi Miyajima[1,*]
[1]Laboratory of Cell Growth and Differentiation, Institute of Molecular and Cellular Biosciences, The University of Tokyo, Tokyo 113-0032, Japan
[2]Department of Host Defense and Biochemical Research, Juntendo University, School of Medicine, Tokyo 113-8421, Japan
[3]Department of Biochemical Science and Technology, National Taiwan University, Taipei 106, Taiwan
*Correspondence: kido@iam.u-tokyo.ac.jp (T.K.), miyajima@iam.u-tokyo.ac.jp (A.M.)
http://dx.doi.org/10.1016/j.stemcr.2015.08.008

SUMMARY

To develop a culture system for large-scale production of mature hepatocytes, liver progenitor cells (LPCs) with a high proliferation potential would be advantageous. We have found that carboxypeptidase M (CPM) is highly expressed in embryonic LPCs, hepatoblasts, while its expression is decreased along with hepatic maturation. Consistently, CPM expression was transiently induced during hepatic specification from human-induced pluripotent stem cells (hiPSCs). CPM$^+$ cells isolated from differentiated hiPSCs at the immature hepatocyte stage proliferated extensively in vitro and expressed a set of genes that were typical of hepatoblasts. Moreover, the CPM$^+$ cells exhibited a mature hepatocyte phenotype after induction of hepatic maturation and also underwent cholangiocytic differentiation in a three-dimensional culture system. These results indicated that hiPSC-derived CPM$^+$ cells share the characteristics of LPCs, with the potential to proliferate and differentiate bi-directionally. Thus, CPM is a useful marker for isolating hiPSC-derived LPCs, which allows development of a large-scale culture system for producing hepatocytes and cholangiocytes.

INTRODUCTION

The liver is a central organ for metabolism, and the parenchymal cells, or hepatocytes, play key roles for homeostasis by expressing numerous metabolic and synthetic enzymes. As they express a number of cytochrome P450 oxidases (CYP450s) responsible for the oxidative biotransformation of many endogenous compounds as well as drugs, primary cultures of hepatocytes have been used for drug discovery and toxicology. However, primary hepatocytes exhibit low metabolic activity in vitro, and the supply of human hepatocytes is also limited and variable. To overcome these challenges, human embryonic stem cells (hESCs) and human-induced pluripotent stem cells (hiPSCs) have been considered as an alternative cell source for production of human hepatocytes. To date, there are many studies reporting hepatic differentiation of hiPSCs/hESCs (Ogawa et al., 2013; Si-Tayeb et al., 2010; Takayama et al., 2012). However, in most cases, differentiation of hepatocytes from hiPSCs is accomplished by a time-consuming culture protocol with multiple differentiation steps using expensive cytokines. Also, hepatocytes derived from hiPSCs possess a limited capacity for proliferation and functional maturation. Thus, it is beneficial to develop a simplified culture system for large-scale production of mature hepatocytes from hiPSCs. As liver progenitor cells (LPCs) such as hepatoblasts proliferate extensively in vitro, it would be useful if such cells could be derived from hiPSCs.

The development of the mouse liver begins with early endoderm development. The cells of the ventral foregut endoderm are induced to the hepatoblast stage by fibroblast growth factor (FGF) and bone morphogenetic protein (BMP) signaling from the heart and septum transversum mesenchyme (STM). Following induction, hepatoblasts proliferate and migrate into the STM to form the liver bud with non-parenchymal cells, such as endothelial progenitor cells and hepatic mesenchymal cells (Zaret and Grompe, 2008). Importantly, hepatoblasts isolated from fetal liver can be cultured long-term while maintaining the potential to differentiate into both hepatocytes and cholangiocytes, two types of liver epithelial cell (Suzuki et al., 2000; Tanimizu et al., 2003). LPCs can also be isolated from normal as well as injured adult livers and maintained in culture for long term, although their role in vivo remains elusive (Miyajima et al., 2014).

It has been reported that LPC-like cells were established from hESCs/hiPSCs (Takayama et al., 2013; Yanagida et al., 2013; Zhao et al., 2009), and these cells were shown to proliferate and differentiate into hepatocyte-like cells or cholangiocyte-like cells. These LPCs were either isolated by cell sorting using a combination of specific cell surface markers or generated by adenovirus-mediated gene transfer to promote hepatic lineage differentiation. To develop an efficient culture system for large-scale production of mature functional hepatocytes, our aim was to identify a specific cell surface marker for isolating hiPSC-derived LPCs. In this study, we identified carboxypeptidase M (CPM) as a cell surface marker for hepatoblasts. CPM was also upregulated in hiPSC-derived cells during hepatic differentiation, and the sorted CPM$^+$ cells

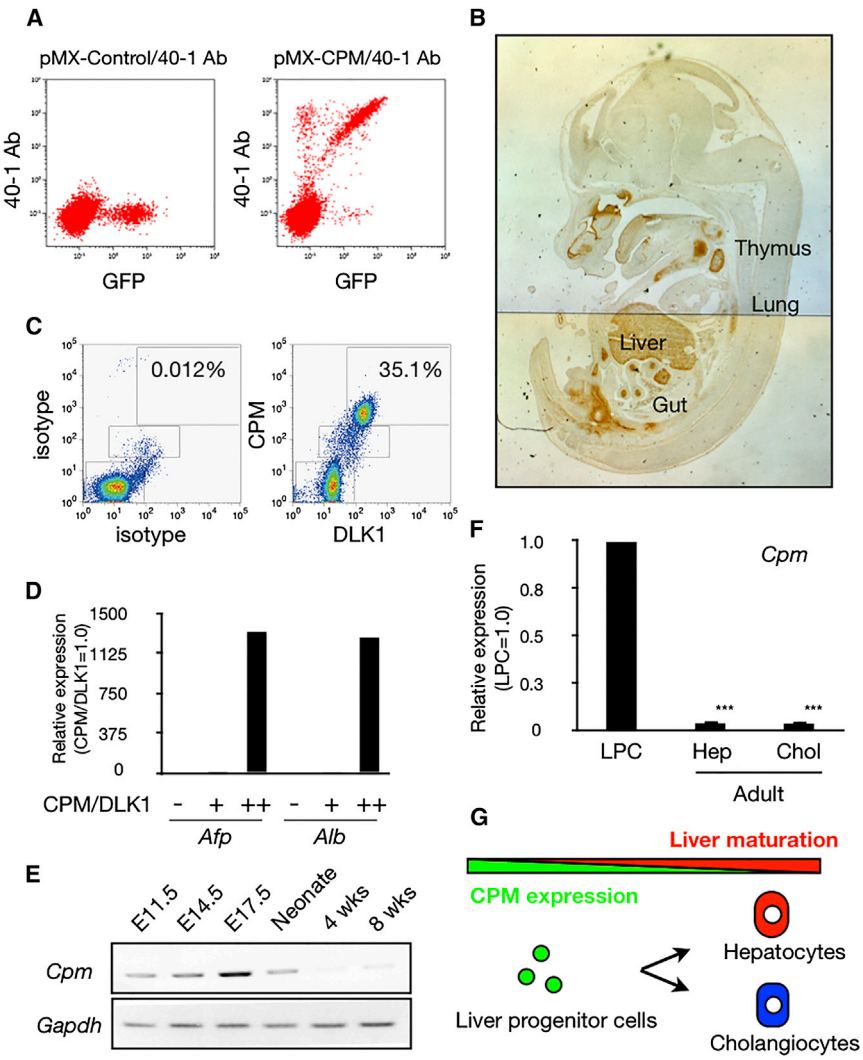

Figure 1. CPM Expression on Mouse Hepatoblasts

(A) FCM analysis of Ba/F3 cells (control) (left) and Ba/F3 cells expressing CPM (right). GFP-positive CPM expressing cells were identified by using the 40-1 antibody.

(B) Localization of CPM (brown) in E14.5 fetal mouse sagittal section.

(C) FCM analysis of mouse fetal liver cells at E14.5 using antibodies against CPM and DLK1.

(D) Relative *Afp* and *Alb* expression in the CPM/DLK1^{neg} (−), CPM/DLK1^{low} (+) and CPM/DLK1^{high} (++) fractions as indicated in (C). n = 1 in each group (each experiment contains two technical replicates).

(E) RT-PCR analysis shows the expression of *Cpm* during mouse liver development (E11.5, E14.5, E17.5, Neonate, 4 weeks, 8 weeks). The product sizes of *Cpm* and *Gapdh* are 430 bp and 600 bp, respectively. Amplification of *Gapdh* was used as an internal control.

(F) Relative *Cpm* expression in liver progenitor cells (LPC), Hep (mature hepatocytes), and Chol (mature cholangiocytes). The results are shown as the mean ± SEM of four independent experiments. (each experiment contains two technical replicates) ***$p < 0.001$.

(G) Correlation between the expression of CPM and the hepatic maturation during liver development.

See also Figure S1 and Table S1.

exhibited features typical of hepatoblasts. Moreover, we developed a highly efficient and reliable culture system for hiPSC-derived LPCs capable of proliferating and differentiating into both hepatocytes and cholangiocytes in vitro.

RESULTS

Identification of CPM as a Hepatoblast Marker

In order to isolate LPCs from hiPSCs effectively, we searched for cell surface molecules expressed in hepatoblasts. Although CXCR4 is known to be expressed in hepatoblasts, it is also detected in endodermal progenitors, thus implying that additional markers would be required to isolate LPCs. DLK1 is an excellent marker for hepatoblasts and has been extensively used to isolate hepatoblasts. However, although immunocytochemical staining using an anti-DLK1 antibody revealed that DLK1-expressing cells were present in hiPSC-derived cells at the immature hepatocyte stage (Figure S1A), flow cytometric (FCM) analysis showed no expression of DLK1 on the cell surface (Figure S1B). We therefore searched for other hepatoblast cell surface molecules. Among 627 monoclonal antibodies established against mouse fetal liver cells (Suzuki et al., 2008), we previously found that 40-1 antibody binds to an unidentified cell surface protein expressed on mouse hepatoblasts (Tanaka et al., 2009). By employing the expression cloning procedure, we identified CPM as the specific antigen for the 40-1 antibody (Figure 1A). Immunohistochemical studies showed that CPM is mainly expressed in endodermal tissues such as liver, thymus, lung, and gut in mouse fetus at E14.5 (Figure 1B), confirming the previous studies that CPM is widely expressed in endodermal tissues during mouse development (Tamplin et al., 2008).

Next, we performed FCM analysis/cell sorting to confirm the expression of CPM in mouse hepatoblasts. CPM was coexpressed with a hepatoblast marker, DLK, and CPM$^+$ cells isolated from E14.5 fetal liver also highly expressed LPC markers such as alpha-1-fetoprotein (*Afp*) and albumin (*Alb*) (Figures 1C and 1D). *Cpm* was highly expressed in fetal liver, but its expression was dramatically decreased after birth (Figure 1E) and was undetectable in mature hepatocytes and cholangiocytes (Figure 1F). Collectively, these data demonstrated that CPM is strongly expressed in hepatoblasts and fetal LPCs (Figure 1G) and also suggested that CPM may be a useful marker for enrichment of LPCs from differentiating hiPSCs.

CPM Expression during Hepatic Differentiation from Human iPSCs

To evaluate whether CPM could be used as a marker for enrichment of LPCs from hiPSCs, we first analyzed the expression levels of *CPM* in human fetal liver. *CPM* was highly expressed in human fetal liver from 6 to 12 weeks of gestation, but was expressed at very low levels in adult liver and HepG2 cells, a human hepatocellular carcinoma cell line (Figure 2A). We then examined the CPM expression profile during hepatic differentiation from hiPSCs by qRT-PCR and FCM analysis. As described in the previously reported protocol, we induced hepatic differentiation in two hiPSC lines (454E2 and 409B2). hiPSCs showed morphological changes after induction toward the hepatic lineage (Figure S2A), with rapid downregulation of OCT4 and sequential induction of GATA4, SOX17, FOXA2, and HNF4α (Figures S2B and S2C). In this culture system, the expression level of *CPM* was undetectable in undifferentiated hiPSCs, but upregulated together with hepatic progenitor markers such as FOXA2 and HNF4α during differentiation (Figures 2B, S2B, and S2C). FCM analysis revealed that 20% of specified hepatic cells were CPM$^+$, with this population increasing to ~40% after differentiation to immature hepatocytes. CPM expression decreased along with subsequent hepatic maturation (Figure 2C). Collectively, these data showed that CPM is a specific cell surface marker for human iPSC-derived LPCs.

Enrichment of hiPSC-Derived LPCs Based on the Expression of CPM

To further characterize the CPM$^+$ cells derived from hiPSCs, we used a magnetic cell sorter to isolate the cells of interest and established a culture system to expand them. The purity of enriched CPM$^+$ cells was over 97% after isolation by single step sorting using a magnetic cell sorter (Figure 2D). CPM$^+$ cells formed compact colonies on MEF feeder cells and exhibited epithelial-like morphology, whereas no such colonies were formed from CPM$^-$ cells (Figure 2E). CPM$^+$ cells exhibited a high proliferative capacity and grew to confluence by day 7 after seeding (Figure 2F). These cells continued to expand after several passages in vitro (Figure 2G). Immunocytochemistry demonstrated that all CPM$^+$ cells strongly expressed AFP and HNF4α, a key transcription factor for LPCs (Figure 2E). These cells could also be cultured even after several passages (Figure S2D) or cryopreservation (Figure S2E). In addition to *AFP* and *HNF4α*, hepatoblast markers *HNF1α*, *PROX1*, *TBX3*, *CD13*, *EpCAM*, and *HHEX* were significantly enriched in CPM$^+$ cells compared with CPM$^-$ cells (Figure 2H). In contrast, *CD133*, a cholangiocyte marker, was significantly expressed in CPM$^-$ cells. All these data strongly suggested that CPM is a useful cell surface marker to enrich for LPCs in hiPSC-derived immature hepatic cells. Similar results were obtained from a different hiPSC line (409B2) (Figure S2F), indicating that the efficiency of our method for generating CPM$^+$ LPCs is not cell line-dependent.

Differentiation of Hepatocytes and Cholangiocytes from CPM$^+$ LPCs

It is well established that LPCs differentiate into both hepatocytes and cholangiocytes. Therefore, we evaluated the differentiation potential of CPM$^+$ LPCs. After expansion of the CPM$^+$ population by serial passages on MEF feeder cells, these cells were then differentiated into hepatocytes by addition of Oncostatin M (Figure 3A). As shown in Figure 3B, the hepatocytes from CPM$^+$ LPCs showed typical human primary hepatocyte morphology, with binuclear cells delineated distinctly by bright borders. In addition, these cells exhibited high level expression of ALB, accumulation of glycogen and uptake of Dil-Ac-LDL (Figures 3C–3E), indicative of mature hepatocytes. FCM analysis showed that almost all differentiated cells expressed ALB (Figure S3A). The levels of hepatic gene expression such as *CYP3A4*, *CYP2C19*, *CYP2C18*, *CYP2D6*, *CYP1A2*, and *CYP2C8* in hepatocyte-like cells derived from CPM$^+$ LPCs were much higher than those derived from hiPSCs by the conventional differentiation protocol (Figure 3F). Furthermore, hepatocytes derived from CPM$^+$ LPCs secreted high amounts of ALB and urea into the culture medium (Figure 3G) and exhibited high CYP3A4 activity (Figure 3H). In addition, CYP3A4 activity was significantly induced in response to rifampicin treatment, which is a well-known CYP3A4 inducer (Figure 3H). Collectively, hepatocytes derived from CPM$^+$ cells exhibited higher metabolic activity compared to those derived from hiPSCs using a conventional protocol.

Furthermore, CPM$^+$ LPCs were converted to cholangiocytes, which formed cysts with the luminal structure in vitro after culturing in a gel consisting of collagen

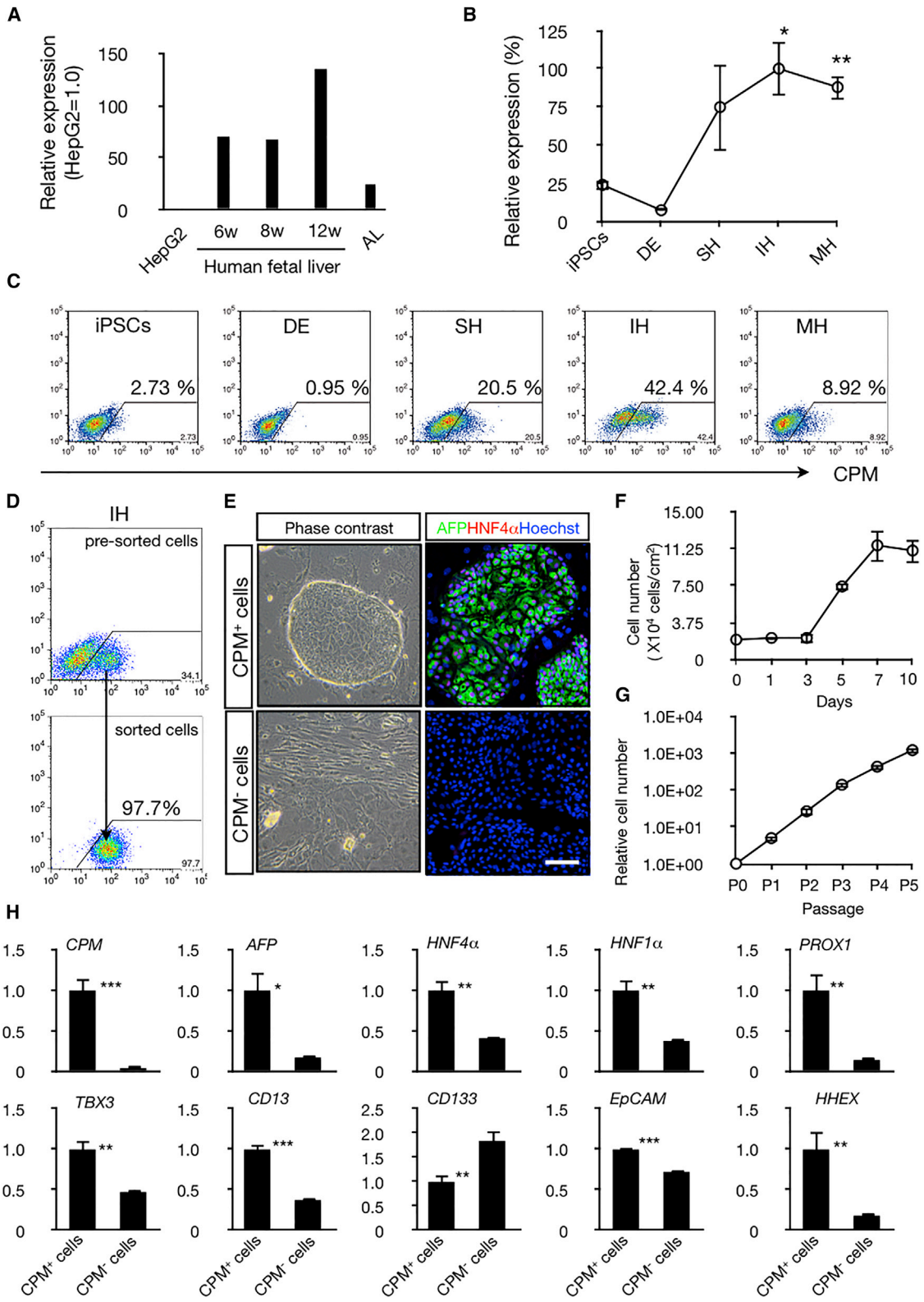

Figure 2. Enrichment of the hiPSC-Derived LPCs Based on the Expression of CPM

(A) Relative *CPM* expression in HepG2 cells and liver tissues (adult liver, gestational ages: 6 weeks, 8 weeks, 12 weeks). n = 1 in each group (each experiment contains two technical replicates).

(legend continued on next page)

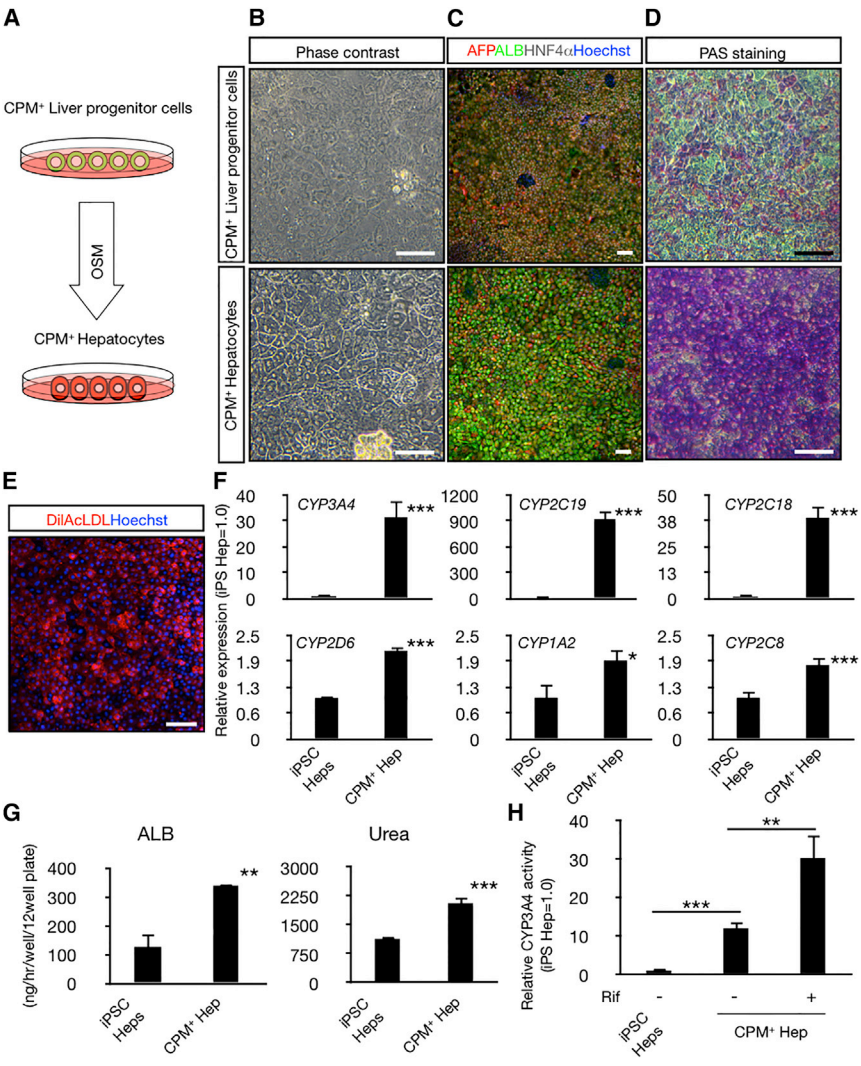

Figure 3. Differentiation of Hepatocytes from hiPSC-Derived CPM$^+$ LPCs

(A) Schematic image of hepatocyte-like cell differentiation from CPM$^+$ LPCs.

(B–D) The morphology of CPM$^+$ LPCs (upper) and CPM$^+$ hepatocyte-like cells (lower) was investigated by microcopy. (B) Phase contrast images. CPM$^+$ LPCs exhibit light cytoplasm and indistinct cell borders. CPM$^+$ hepatocyte-like cells exhibit cobblestone-like morphology with binucleation. (C) Immunohistochemistry for AFP (red), ALB (green) and HNF4α (gray). Nuclei were counterstained with Hoechst 33342 (blue). (D) PAS staining showed accumulation of glycogen. Scale bars, 100 μm.

(E) Uptake of DiIAcLDL (red) in CPM$^+$ hepatocyte-like cells. Scale bar, 100 μm.

(F) qRT-PCR analysis of various CYP450s mRNA levels. The results are shown as the mean ± SEM of six independent experiments. (each experiment contains two technical replicates). iPSC-Heps was used as a control. *p < 0.05, **p < 0.01, ***p < 0.001.

(G) Secretion of ALB and urea. The results are shown as the mean ± SEM of seven independent experiments. iPSC-Heps was used as a control. *p < 0.05, **p < 0.01, ***p < 0.001.

(H) Relative CYP3A4 activity. The results are shown as the mean ± SEM of at least three independent experiments. Treatment with 10 μM of rifampicin (Rif) for 72 hr. iPSC-Heps was used as a control. *p < 0.05, **p < 0.01, ***p < 0.001.

See also Figure S3 and Tables S1 and S2.

and Matrigel (Figures 4A, 4B, S4A, and S4B). The expression of *AFP* was dramatically decreased after differentiation (Figure 4C). Moreover, immunohistochemistry showed that F-actin, PKC, and AQP1 localized to the apical membrane, whereas CD49f was detected in the basolateral membrane in cystic cells (Figures 4D–4F), thus

(B and C) CPM mRNA and protein expression were analyzed by qRT-PCR (B) and FCM (C). iPSCs, iPS cells; DE, definitive endoderm; SH, specified hepatic; IH, immature hepatocytes; MH, mature hepatocytes. For (B), error bar represents the mean ± SEM of three independent experiments. *p < 0.05 between iPSCs and IH, **p < 0.01 between iPSCs and MH. See also Figures S2B and S2C.

(D) FCM analysis of CPM expression was performed in pre- and post-sorted cells.

(E) Morphology of the CPM$^+$ cells (left upper) and CPM$^-$ cells (left lower) on MEF feeder cells. Cells were cultured for 4 days. Immunohistochemical staining for AFP (green) and HNF4α (red) in CPM$^+$ cells (right upper) and CPM$^-$ cells (right lower). Nuclei were visualized by Hoechst 33342 staining (blue). Scale bar, 100 μm.

(F) Growth curve of CPM$^+$ cells. Each value was determined in triplicate. Error bar represents the mean ± SEM of three independent experiments.

(G) Relative cell number after several passages. Error bar represents the mean ± SEM of four independent experiments.

(H) Expression of hepatoblast markers in CPM$^+$ cells compared with CPM$^-$ cells. *p < 0.05, **p < 0.01, ***p < 0.001. The results are shown as the mean ± SEM of eight independent experiments. (each experiment contains two technical replicates).

See also Tables S1and S2.

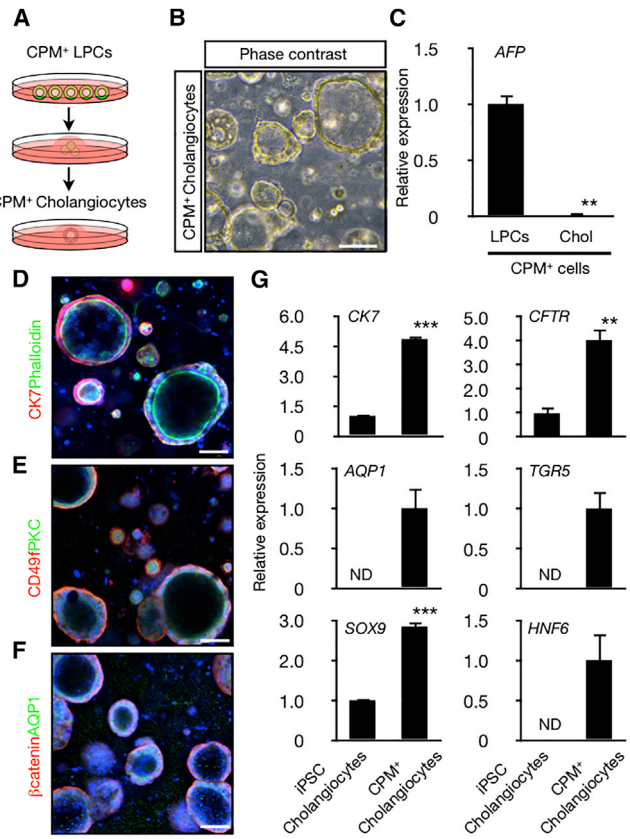

Figure 4. Differentiation of Cholangiocytes from hiPSC-Derived CPM+ LPCs

(A) Schematic image of cholangiocyte-like cells differentiation from CPM+ LPCs.

(B) Phase contrast image. CPM+ LPCs form cysts in collagen/Matrigel after 7 days of culture. See also Figures S4A and S4B.

(C) Expression of *AFP* in CPM+ LPCs and CPM+ cholangiocytes. The results are shown as the mean ± SEM of four independent experiments (each experiment contains two technical replicates). **p < 0.01.

(D–F) Immunofluorescence staining for cholangiocyte markers in CPM+ cholangiocyte-like cells. Localization of (D) CK7 (red), F-actin (green), (E) CD49f (red), PKC (green), (F) β-catenin (red), AQP1 (green). Nuclei were visualized by Hoechst 33342 staining (blue). Scale bars, 100 μm.

(G) Gene expression profile of CPM+ cholangiocyte-like cells compared with iPSC cholangiocyte-like cells. The results are shown as the mean ± SEM of four independent experiments (each experiment contains two technical replicates). ND, not detected. **p < 0.01, ***p < 0.001.

See also Tables S1 and S2.

showing the proper apico-basal structure. In this culture system, cells derived from CPM+ LPCs highly expressed cholangiocyte marker genes, such as *CK7*, *CFTR*, *AQP1*, *TGR5*, *SOX9*, and *HNF6*, compared with iPSC-derived cholangiocytes (without CPM purification process) (Figure 4G). These results indicate that CPM+ LPCs can differentiate into both hepatocyte-like cells and cholangiocyte-like cells.

DISCUSSION

Generation of mature hepatocytes and cholangiocytes from iPS/ES cells requires time-consuming multiple processes with expensive cytokines. Therefore, it would be beneficial to derive expandable precursor cells to simplify the procedure. Because LPCs are able to proliferate extensively in vitro and differentiate to both hepatocytes and cholangiocytes (Suzuki et al., 2000; Tanimizu et al., 2003, 2007), they are ideal cells to use in developing an efficient protocol for large-scale production of mature liver cells. In order to isolate LPCs, we first tested the expression of DLK1 and CXCR4, which are well known to be expressed in hepatoblasts. However, neither of these markers was appropriate for enriching LPCs from hiPSC-derived cells, as described above. We therefore searched for another marker and showed that CPM is a cell surface antigen expressed on hepatoblasts in mouse fetal liver between E11.5 and E17.5, although its expression is dramatically downregulated in mature hepatocytes and cholangiocytes. CPM is a member of the carboxypeptidase family, expressed on the cell surface to catalyze the release of C-terminal arginine or lysine residues of peptides and proteins (Skidgel et al., 1989). While its role in hepatoblasts is currently unknown, we found that the expression of CPM was gradually upregulated along with hepatic differentiation from hiPSC-like liver development. The simple method of single step cell sorting based on CPM expression made it possible to enrich the LPC fraction after induction of hiPSCs to the immature hepatocyte stage. These CPM+ cells exhibited a high proliferative potential and the expanded cells could be cryopreserved. Moreover, they expressed various liver progenitor markers (Figure 2H). While most CPM+ cells expressed HNF4α (Figure 2E), expression of midgut/hindgut markers such as *CDX2* and *PDX1* was also detected by RT-PCR (data not shown), suggesting that CPM+ cells may contain non-liver progenitors. However, after induction of hepatic differentiation, almost all cells became hepatocytes as shown by their morphology and ALB expression (Figures 3B, 3C, and S3A). If such non-hepatic progenitors were present in the CPM+ cells, they did not affect hepatocyte differentiation.

CPM+ LPCs were able to differentiate in a single step culture to either hepatocyte-like cells or cholangiocyte-like cells depending on the culture condition. Furthermore, hepatocytes derived from CPM+ cells exhibited a

significantly higher level of metabolic activity compared to the hiPSC-derived hepatocytes using a conventional differentiation protocol. Importantly, these hepatocyte-like cells remain phenotypically stable for more than 2 weeks (Figure S3B). Thus, CPM$^+$ LPCs derived from hiPSCs will be useful for developing a reliable long-term hepatocyte culture system, and this simplified purification method will contribute to basic and clinical research related to liver diseases. Although CPM$^+$ hepatocytes highly expressed mature hepatic genes involved in gluconeogenesis (*G6PC*, *PCK1*) and the urea cycling (*CPS1*), they exhibited variable levels of CYP expression compared with cultured primary human hepatocytes (Figure S3C). It is well known that the capacity to metabolize drugs is variable due to genetic polymorphisms in CYPs (Ingelman-Sundberg et al., 2007). Hepatocyte-like cells differentiated from iPSCs are highly variable due to retention of donor-specific metabolic capacity (Takayama et al., 2014), suggesting that the expression of CYPs in CPM$^+$ Hepatocytes may be affected by a donor's genetic background.

Because freshly isolated hepatocytes rapidly lose their functions, it is a major challenge to generate fully functional hepatocytes from pluripotent stem cells. While hepatocytes derived from CPM$^+$ LPCs expressed high levels of metabolic activity, the levels of some proteins are not as high as primary human hepatocytes and there is still room for improvement. During embryogenesis, hepatoblasts differentiate into mature hepatocytes through interactions with non-parenchymal cells. As non-parenchymal cells are in direct contact with hepatoblasts and also produce various cytokines to induce hepatic maturation, co-culture of CPM$^+$ hepatocytes with non-parenchymal cells may be an effective way to generate more mature hepatocytes from hiPSCs, and we are currently investigating this possibility.

EXPERIMENTAL PROCEDURES

Cell Culture

Two hiPSC lines (454E2 and 409B2) were provided by RIKEN Cell Bank (Okita et al., 2011). These cells were maintained on mitomycin C-treated (Wako Pure Chemical Industries) mouse embryonic fibroblast (MEF) feeder cells, and hepatic differentiation of hiPSCs was induced using the four-step protocol previously reported, with minor modifications (Si-Tayeb et al., 2010).

Isolation and Expansion of LPCs Derived from hiPSCs

After induction of hiPSCs to the immature hepatocyte stage, cells were sorted using a MoFlo XDP cell sorter (Beckman Coulter) or autoMACS Pro Separator (Miltenyi Biotech) into CPM$^+$ and CPM$^-$ populations. To expand hiPSC-derived CPM$^+$ cells, we modified the published method (Chen et al., 2007; Huch et al., 2013; Yanagida et al., 2013) as follows: sorted cells were cultured on mitomycin c-treated MEF feeder cells (2.0×10^4 cells/cm^2) in DMEM-F12 (Sigma-Aldrich) supplemented with 10% FBS (JRH Biosciences), penicillin-streptomycin-glutamine, ITS, N-2 supplement, MEM non-essential amino acids solution, L-glutamine (Life Technologies), ascorbic acid (1 mM), nicotinamide (10 mM), N-acetylcysteine (0.2 mM) (Sigma-Aldrich), dexamethasone (1×10^{-7} M), HGF (20 ng/ml), EGF (10 ng/ml) (PeproTech), Y-27632 (5 μM) (Wako), and A83-01 (2.5 μM) (Tocris).

Differentiation of Hepatocytes and Cholangiocytes from CPM$^+$ LPCs

To induce hepatic maturation of CPM$^+$ LPCs, confluent cells were incubated in Hepatocyte Basal Medium (Lonza) supplemented with HCM SingleQuots (excluding EGF) and Oncostatin M (20 ng/ml) (PeproTech) for 5–10 days as described previously (Si-Tayeb et al., 2010). Induction of cholangiocyte differentiation was performed using the three-dimensional gel culture method previously reported (Tanimizu et al., 2007; Yanagida et al., 2013) with minor modifications. After expansion of CPM$^+$ LPCs, the resulting cells were collected and re-suspended in a gel composed of 2:3 mixture of growth factor reduced Matrigel (Corning) and collagen type I (Nitta Gelatin) at a density of 1×10^5 cells/50 μl. Cell suspensions were then added to a 24-well plate (Corning) and incubated for 2 hr at 37°C until solidification. The cells were then cultured in the presence of R-spondin-1 (40 ng/ml) and WNT-3a (40 ng/ml) (PeproTech) for 7 days.

Additional details of experimental procedures are available in the Supplemental Information.

SUPPLEMENTAL INFORMATION

Supplemental Information includes Supplemental Experimental Procedures, four figures, and two tables and can be found with this article online at http://dx.doi.org/10.1016/j.stemcr.2015.08.008.

AUTHOR CONTRIBUTIONS

T.K. designed the study, performed experiments, analyzed data, and wrote the manuscript. Y.K., K.S., A.K., Y.M., and E.C. performed experiments and analyzed data. M.T. designed the study, performed experiments, and analyzed data. A.M. designed the study, analyzed data, and wrote the manuscript.

ACKNOWLEDGMENTS

We thank Drs. Yasuyuki Sakai (CIBiS, Institute of Industrial Science, The University of Tokyo) and Takahiro Ochiya (Division of Molecular and Cellular Medicine, National Cancer Center Research Institute) for helpful discussions, and Dr. Cindy Kok for critical review of the manuscript. This study was supported by CREST program of Japan Science and Technology Agency, and Grants-in-Aid for Scientific Research of Japan Society for the Promotion of Science.

Received: April 8, 2015
Revised: August 7, 2015
Accepted: August 8, 2015
Published: September 10, 2015

REFERENCES

Chen, Q., Kon, J., Ooe, H., Sasaki, K., and Mitaka, T. (2007). Selective proliferation of rat hepatocyte progenitor cells in serum-free culture. Nat. Protoc. *2*, 1197–1205.

Huch, M., Dorrell, C., Boj, S.F., van Es, J.H., Li, V.S., van de Wetering, M., Sato, T., Hamer, K., Sasaki, N., Finegold, M.J., et al. (2013). In vitro expansion of single Lgr5^{+} liver stem cells induced by Wnt-driven regeneration. Nature *494*, 247–250.

Ingelman-Sundberg, M., Sim, S.C., Gomez, A., and Rodriguez-Antona, C. (2007). Influence of cytochrome P450 polymorphisms on drug therapies: pharmacogenetic, pharmacoepigenetic and clinical aspects. Pharmacol. Ther. *116*, 496–526.

Miyajima, A., Tanaka, M., and Itoh, T. (2014). Stem/progenitor cells in liver development, homeostasis, regeneration, and reprogramming. Cell Stem Cell *14*, 561–574.

Ogawa, S., Surapisitchat, J., Virtanen, C., Ogawa, M., Niapour, M., Sugamori, K.S., Wang, S., Tamblyn, L., Guillemette, C., Hoffmann, E., et al. (2013). Three-dimensional culture and cAMP signaling promote the maturation of human pluripotent stem cell-derived hepatocytes. Development *140*, 3285–3296.

Okita, K., Matsumura, Y., Sato, Y., Okada, A., Morizane, A., Okamoto, S., Hong, H., Nakagawa, M., Tanabe, K., Tezuka, K., et al. (2011). A more efficient method to generate integration-free human iPS cells. Nat. Methods *8*, 409–412.

Si-Tayeb, K., Noto, F.K., Nagaoka, M., Li, J., Battle, M.A., Duris, C., North, P.E., Dalton, S., and Duncan, S.A. (2010). Highly efficient generation of human hepatocyte-like cells from induced pluripotent stem cells. Hepatology *51*, 297–305.

Skidgel, R.A., Davis, R.M., and Tan, F. (1989). Human carboxypeptidase M. Purification and characterization of a membrane-bound carboxypeptidase that cleaves peptide hormones. J. Biol. Chem. *264*, 2236–2241.

Suzuki, A., Zheng, Y., Kondo, R., Kusakabe, M., Takada, Y., Fukao, K., Nakauchi, H., and Taniguchi, H. (2000). Flow-cytometric separation and enrichment of hepatic progenitor cells in the developing mouse liver. Hepatology *32*, 1230–1239.

Suzuki, K., Tanaka, M., Watanabe, N., Saito, S., Nonaka, H., and Miyajima, A. (2008). p75 Neurotrophin receptor is a marker for precursors of stellate cells and portal fibroblasts in mouse fetal liver. Gastroenterology *135*, 270–281.e3.

Takayama, K., Inamura, M., Kawabata, K., Sugawara, M., Kikuchi, K., Higuchi, M., Nagamoto, Y., Watanabe, H., Tashiro, K., Sakurai, F., et al. (2012). Generation of metabolically functioning hepatocytes from human pluripotent stem cells by FOXA2 and HNF1α transduction. J. Hepatol. *57*, 628–636.

Takayama, K., Nagamoto, Y., Mimura, N., Tashiro, K., Sakurai, F., Tachibana, M., Hayakawa, T., Kawabata, K., and Mizuguchi, H. (2013). Long-term self-renewal of human ES/iPS-derived hepatoblast-like cells on human laminin 111-coated dishes. Stem Cell Reports *1*, 322–335.

Takayama, K., Morisaki, Y., Kuno, S., Nagamoto, Y., Harada, K., Furukawa, N., Ohtaka, M., Nishimura, K., Imagawa, K., Sakurai, F., et al. (2014). Prediction of interindividual differences in hepatic functions and drug sensitivity by using human iPS-derived hepatocytes. Proc. Natl. Acad. Sci. USA *111*, 16772–16777.

Tamplin, O.J., Kinzel, D., Cox, B.J., Bell, C.E., Rossant, J., and Lickert, H. (2008). Microarray analysis of Foxa2 mutant mouse embryos reveals novel gene expression and inductive roles for the gastrula organizer and its derivatives. BMC Genomics *9*, 511.

Tanaka, M., Okabe, M., Suzuki, K., Kamiya, Y., Tsukahara, Y., Saito, S., and Miyajima, A. (2009). Mouse hepatoblasts at distinct developmental stages are characterized by expression of EpCAM and DLK1: drastic change of EpCAM expression during liver development. Mech. Dev. *126*, 665–676.

Tanimizu, N., Nishikawa, M., Saito, H., Tsujimura, T., and Miyajima, A. (2003). Isolation of hepatoblasts based on the expression of Dlk/Pref-1. J. Cell Sci. *116*, 1775–1786.

Tanimizu, N., Miyajima, A., and Mostov, K.E. (2007). Liver progenitor cells develop cholangiocyte-type epithelial polarity in three-dimensional culture. Mol. Biol. Cell *18*, 1472–1479.

Yanagida, A., Ito, K., Chikada, H., Nakauchi, H., and Kamiya, A. (2013). An in vitro expansion system for generation of human iPS cell-derived hepatic progenitor-like cells exhibiting a bipotent differentiation potential. PLoS ONE *8*, e67541.

Zaret, K.S., and Grompe, M. (2008). Generation and regeneration of cells of the liver and pancreas. Science *322*, 1490–1494.

Zhao, D., Chen, S., Cai, J., Guo, Y., Song, Z., Che, J., Liu, C., Wu, C., Ding, M., and Deng, H. (2009). Derivation and characterization of hepatic progenitor cells from human embryonic stem cells. PLoS ONE *4*, e6468.

Stem Cell Reports, Volume *5*

Supplemental Information

CPM Is a Useful Cell Surface Marker to Isolate Expandable Bi-Potential Liver Progenitor Cells Derived from Human iPS Cells

Taketomo Kido, Yuta Koui, Kaori Suzuki, Ayaka Kobayashi, Yasushi Miura, Edward Y. Chern, Minoru Tanaka, and Atsushi Miyajima

Supplemental Information

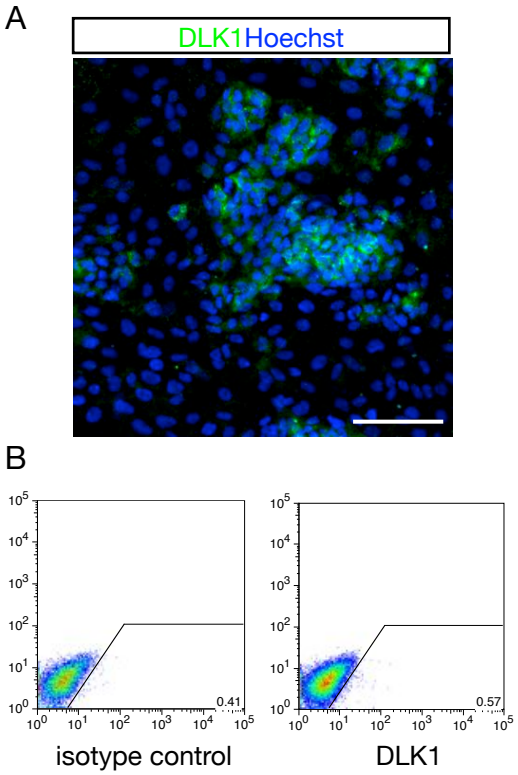

Figure S1. DLK1 expression during hepatic differentiation from hiPSCs, related to Figure 1

(A) Immunofluorescence analysis for DLK1 (green) in the hiPSC-derived immature hepatocyte stage. Nuclei were counterstained with Hoechst 33342 (blue). (B) FCM analysis for DLK1 expression.

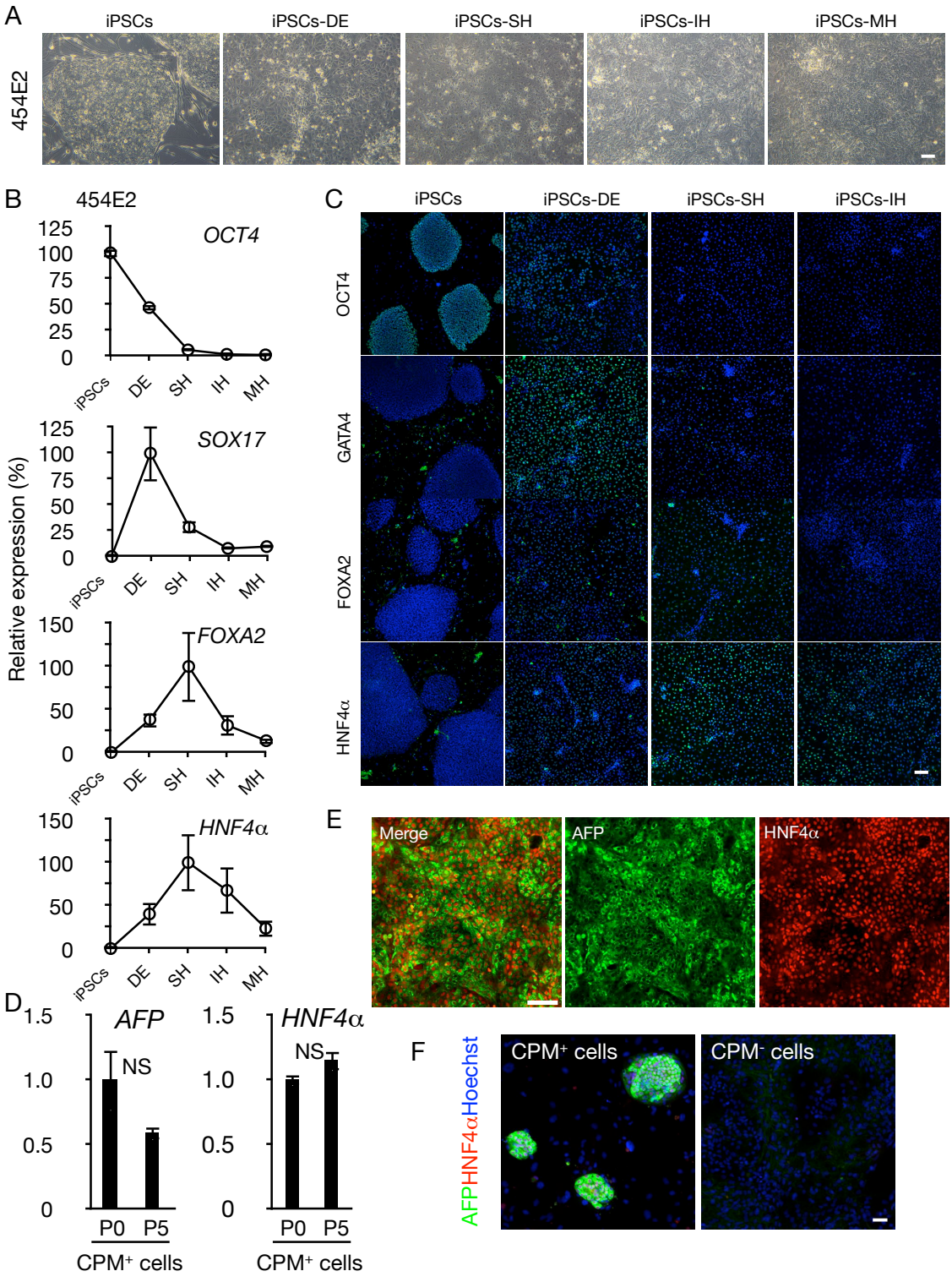

Figure S2. Induction of hepatic differentiation from hiPSCs, related to Figure 2

(A) Morphological changes of hiPSCs at different stages of hepatic differentiation. Scale bar, 100 μm. (B) Quantitative RT-PCR analysis for *OCT4*, *SOX17*, *FOXA2* and *HNF4α*. Error bar represents the mean ± SEM of 3 independent experiments. (each experiment contains 2 technical replicates) (C) Immunofluorescence analysis for OCT4, GATA4, FOXA2 and HNF4 α (green). Nuclei were counterstained with Hoechst 33342 (blue). Scale bar, 100 μm. (D) Expression of hepatoblast markers in CPM^+ LPCs. The results are shown as the mean ± SEM of 6 independent experiments. P0: passage 0, P5: passage 5. NS, no significance. (each experiment contains 2 technical replicates) (E) Immunofluorescence analysis for AFP (green) and HNF4 α (red) in CPM^+ LPCs after cryopreservation. (F) Immunofluorescence analysis shows the expression of AFP (green) and HNF4 α (red) in CPM^+ LPCs derived from 409B2 line. Nuclei were visualized by Hoechst 33342 staining (blue). Scale bar, 100 μm.

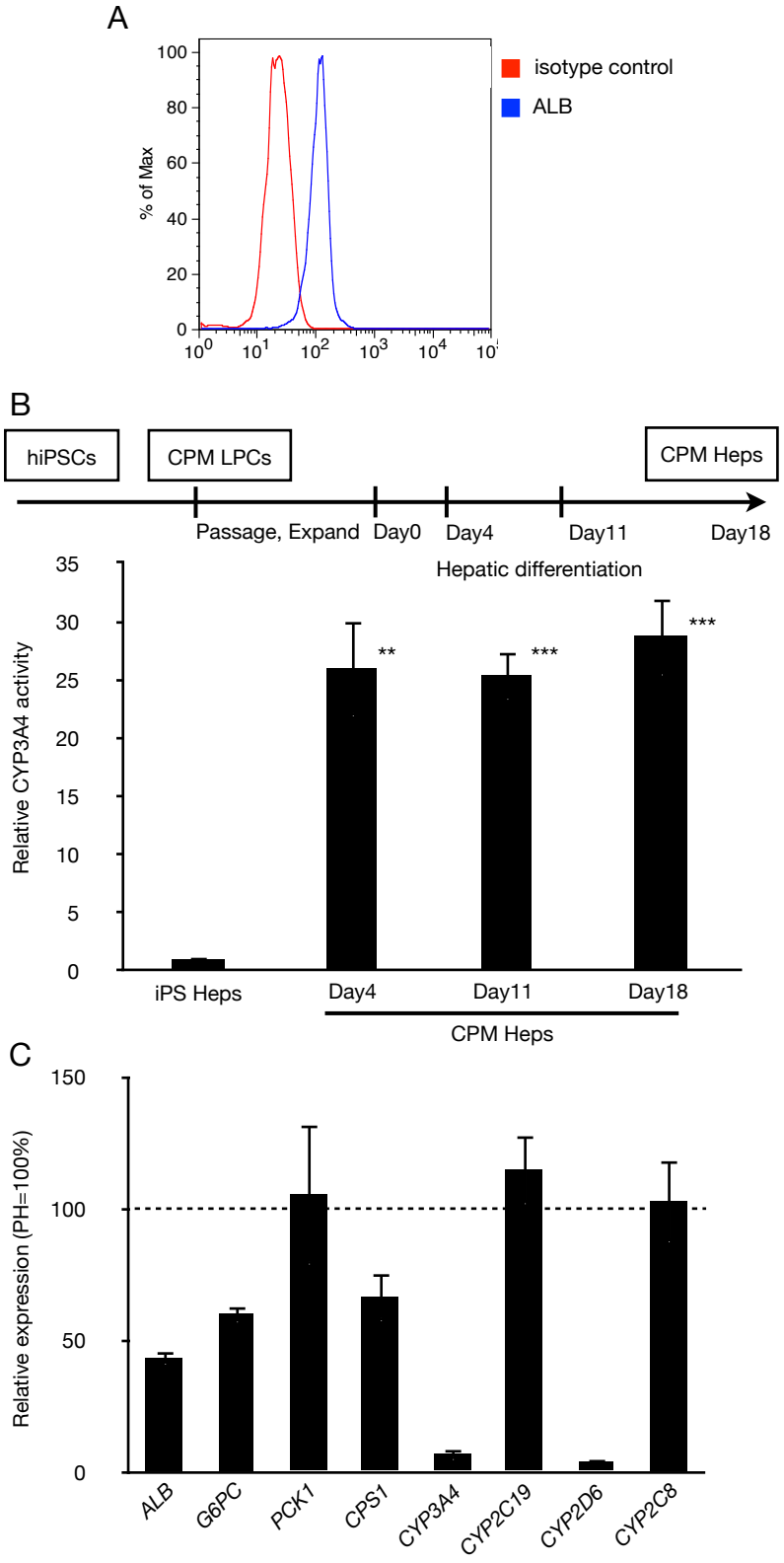

Figure S3. Differentiation of hepatocytes from CPM$^+$ LPCs, related to Figure 3

(A) FCM analysis for ALB. (B) CYP3A4 activities in the culture of CPM^+ hepatocytes at day 0, 4, 18. The results are shown as the mean ± SEM of independent experiments. n=8, 6, 6, 6 in each group. **P<0.01, ***P<0.001 (C) Relative *ALB*, *G6PC*, *PCK1*, *CPS1*, *CYP3A4*, *CYP2C19*, *CYP2D6* and *CYP2C8* expressions in the CPM^+ hepatocytes compared with primary human hepatocytes (PH). The results are shown as the mean ± SEM of independent experiments. n=6. (each experiment contains 2 technical replicates)

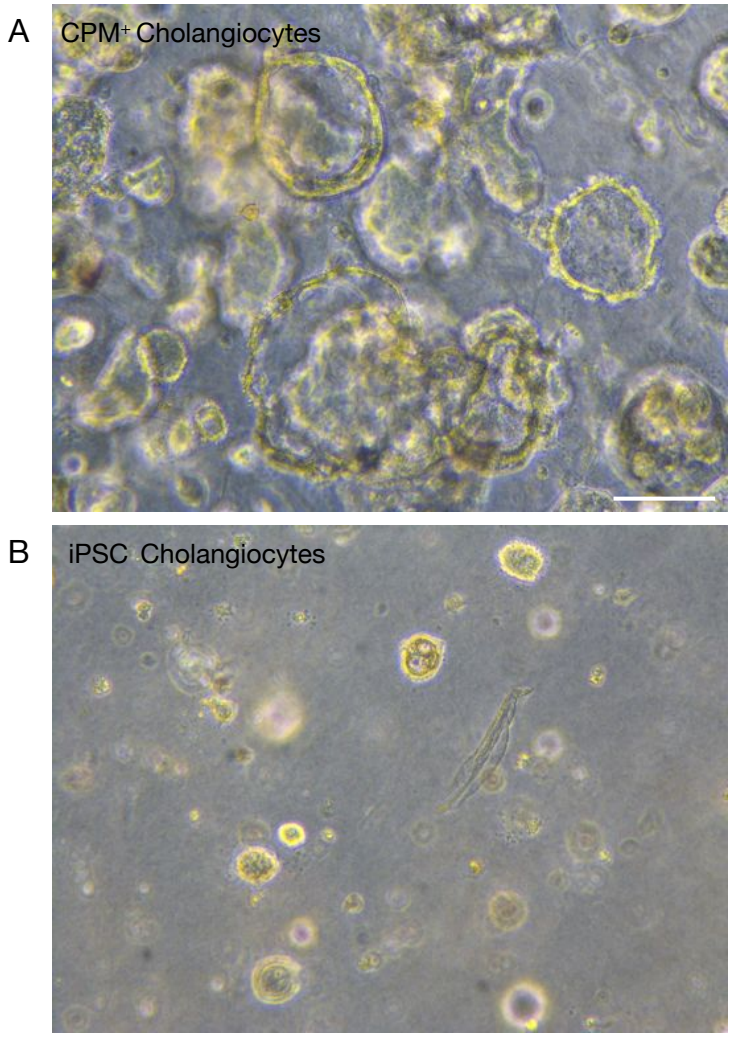

Figure S4. Differentiation of cholangiocytes from CPM$^+$ LPCs, related to Figure 4

(A, B) Phase contrast images. CPM$^+$ cholangiocytes (A) and iPSC cholangiocytes (without CPM purification process) (B). Scale bar, 100 μm.

Table S1. List of Quantitative RT-PCR primers for mouse and human genes, related to Figures 1-4, S2 and S3

	Left primer	Right primer	Product size
Actb	TTCTTTGCAGCTCCTTCGTT	ATGGAGGGGAATACAGCCC	149
Afp	GGCGATGGGTGTTTAGAAAG	CAGCAGCCTGAGAGTCCATA	95
Alb	TGCACACTTCCAGAGAAGGA	GTCTTCAGTTGCTCCGCTGT	98
Cpm	CCCGTTTAGAACCAACAAGC	GAGTCGTGTCCAGGGACTGT	78

	Left primer	Right primer	Product size
ACTB	GCACAGAGCCTCGCCTT	GTTGTCGACGACGAGCG	93
AFP	AGAGGAGATGTGCTGGATTG	GTGGTCAGTTTGCAGCATTC	110
ALB	TGCTGATGAGTCAGCTGAAAA	TCAGCCATTTCACCATAGGTT	105
OCT4	GAAGGAGAAGCTGGAGCAAA	CTTCTGCTTCAGGAGCTTGG	94
SOX17	CAGAATCCAGACCTGCACAA	TCTGCCTCCTCCACGAAG	101
FOXA2	CGACTGGAGCAGCTACTATGC	TGTTGCTCACGGAGGAGTAG	90
HNF4α	GCAGGCTCAAGAAATGCTTC	GGCTGCTGTCCTCATAGCTT	102
CPM	GGATGGAAGCGTTTTTGAAG	CCACAACAAGAACCCACAGG	108
CYP3A4	TTTTGTCCTACCATAAGGGCTTT	CACAGGCTGTTGACCATCAT	95
CYP2C19	TTGCTTCCTGATCAAAATGG	GTCTCTGTCCCAGCTCCAAG	108
CYP2C18	ATGAACAGTGCTCGGGACTT	TGGCTATCAAGCTTTCAACAG	100
CYP2D6	TGGACTTCCAGAACACACCA	CCCATTGAGCACGACCAC	104
CYP1A2	CTTCGTAAACCAGTGGCAGG	AGGGCTTGTTAATGGCAGTG	110
CYP2C8	CTCGGGACTTTATGGATTGC	CAGTGCCAACCAAGTTTTCA	93
CK7	CTGCCTACATGAGCAAGGTG	GGGACTGCAGCTCTGTCAAC	108
AQP1	CTCTCAGGCATCACCTCCTC	GGAGGGTCCCGATGATCT	109
CFTR	ACAGAAGCGTCATCAAAGCA	CCACTCAGTGTGATTCCACCT	100
SOX9	GACGCTGGGCAAGCTCT	GTAATCCGGGTGGTCCTTCT	106
HNF1α	CCTCAAAGAGCTGGAGAACCT	GACTTGACCATCTTCGCCAC	108
PROX1	ACAGGGCTCTGAACATGCAC	GGCATTGAAAAACTCCCGTA	101
TBX3	CTTCCACCTCCAGCAGCA	GCCATGTACGTGTAGGGGTA	90
CD13	AACCTCATCCAGGCAGTGAC	AAGCCTGTTTCCTCGTTGTC	92
CD133	CCATTGGCATTCTCTTTGAA	TTTGGATTCATATGCCTTCTGT	110
EpCAM	CTGAATTCTCAATGCAGGGTC	CCCATCTCCTTTATCTCAGCC	148
HHEX	CCTCTGTACCCCTTCCCG	GGGGCTCCAGAGTAGAGGTT	90
TGR5	CAGCAACTCCCTGACACTCA	TCTTGGTCCTGGGGACAG	110
HNF6	GGAGGATGTGGAAGTGGCT	TGTTGCCTCTATCCTTCCCA	108

Table S2. List of 1st and 2nd antibodies used for this study, related to Figures 2-4 and S2

Primary antibodies

	Species	Company (catalogue number)
AFP	Rabbit	Dako (A000829)
AFP	Mouse	Sigma-Aldrich (A8452)
ALB	Rabbit	Dako (A0001)
ALB	Mouse	Nippon bio-test laboratories (0902-1)
HNF4α	Goat	SantaCruz (sc-6556)
CK7	Mouse	Dako (M7018)
CD49f	Rat	BD Pharmingen (555734)
PKC	Rabbit	SantaCruz (sc-216)
CTNNB1	Mouse	BD Pharmingen (610153)
AQP1	Rabbit	SantaCruz (sc-20810)
OCT4	Rabbit	SantaCruz (sc-9081)
GATA4	Goat	SantaCruz (sc-1237)
FOXA2	Goat	SantaCruz (sc-6554)

Secondary antibodies

	Species	Company (catalogue number)
Alexa Fluor 488 anti-Rabbit IgG	Donkey	Life technologies (A21206)
Alexa Fluor 488 anti-Goat IgG	Donkey	Life technologies (A11055)
Alexa Fluor 555 anti-Goat IgG	Donkey	Life technologies (A21432)
Alexa Fluor 555 anti-Mouse IgG	Donkey	abcam (ab150110)
Alexa Fluor 647 anti-Goat IgG	Donkey	Life technologies (A21447)

Supplemental experimental procedures

Animals

C57BL/6 mice were used in the present study. All animal experiments were approved by the institutional Animal Care and Use Committee of the University of Tokyo.

Human primary hepatocyte culture

Human cryopreserved hepatocytes and all cell culture media were purchased from Biopredic International (Rennes, France). Hepatocytes were cultured according to the manufacturer's protocol. Briefly, hepatocytes were thawed using thawing medium and seeded at a density of 0.4 x 10^6 cells/well onto 24-well collagen I coated plates in seeding medium. After 1 day of culture, the medium was replaced with incubation medium and culture continued for 5 days.

Analysis of mouse fetal liver cells

Mouse fetal livers were collected from C57BL/6 mice at E14.5. The livers were minced and dissociated in Liver Digest Medium (Life technologies, California, US) for 15 min. The fetal liver cell suspension was passed through a 40 μm cell strainer (BD Biosciences, New Jersey, US) to obtain a single cell suspension. Then, cells were blocked by Fc block reagent and incubated with PE-conjugated anti-CPM antibody and FITC-conjugated anti-DLK1 antibody. PE and FITC-conjugated isotype controls were used as negative controls. CPM-positive (CPM^+) and -negative (CPM^-) cells were isolated by a MoFlo XDP cell sorter (Beckman Coulter, Inc, California, US).

Quantitative RT-PCR

Human fetal and adult liver RNAs were obtained from Gene Technology, Inc. (St. Louis, Missouri, US) and Life technologies, respectively.

Total RNA from cells was extracted with TRIzol reagent (Life technologies) according to the manufacturer's protocol. First-strand cDNA was synthesized using the PrimeScriptII 1st strand cDNA Synthesis Kit (Takara bio, Shiga, Japan). Quantitative RT-PCR was performed with the cDNA using specific primers for mouse and human genes. All data were calculated using the ddCt method with β-actin as a normalization control. Primers are listed in the Table S1.

Flow cytometric analysis for hiPSCs

Flow cytometric analysis was used to detect CPM^+ or $DLK1^+$ cells. Cells were dissociated using 0.05% trypsin/0.5 mM EDTA solution and then resuspended in PBS containing 0.03% BSA (PBS-BSA). Cells were incubated for 20 min with FcR blocking reagent (Miltenyi Biotech, Bergisch-Gladbach, Germany) followed by incubation with anti-Carboxypeptidase M antibody (Abcam, Massachusetts, US) or anti-DLK1 antibody (LivTech, Kanagawa, Japan) for 30 min on ice. Purified Mouse IgG1 isotype control (BioLegend, California, US) was used as negative control. Cells were washed and labeled with PE-conjugated anti-mouse IgG1 (BioLegend) for 30 min on ice.

Growth rate of CPM^+ cells

After the CPM^+ cells reached 50% confluence, they were passaged onto mitomycin C-treated MEF feeder cells. Cells were seeded into each well of a 12-well plate (Corning, New York, US) at 2.0 x 10^4 cells/cm^2. Cell proliferation was monitored in triplicate using a hemocytometer.

Immunohistochemistry and Immunocytochemistry

Fetal mouse was embedded in OCT compound (Sakura Finetek Japan., Co., Ltd., Tokyo, Japan). 10 μm sections were prepared and mounted on glass slides coated with APS (Matsunami glass Ind. Ltd., Osaka, Japan). Sections were fixed in 4% paraformaldehyde solution in PBS for 10 min, and washed three times with PBS. The sections were treated with 3% hydrogen peroxide (Wako Pure Chemical Industries, Ltd.) in methanol for 20 min. After washing three times with PBS, sections were blocked for 20 minutes with 4% skim milk in PBS and then incubated with anti-CPM antibody in a moisture chamber at 4°C overnight. They were again washed three times in PBS and incubated with biotinylated secondary antibody for 40 min at room temperature. Then, the sections were treated with an ABC-PO kit (Vector Laboratories Inc., California, US) for 1 hr at room temperature. Finally, the immunoreactive cells were visualized by 3,3'-diaminobenzidine tetra-hydrochloride (Dojin Laboratories, Kumamoto, Japan) and then counterstained with Hematoxylin (MERCK, Darmstadt, Germany) for 5 min.

Cultured cells were fixed in 10% buffered formalin solution (Wako Pure Chemical Industries, Ltd.) at room temperature for 10 minutes, and washed three times with PBS. Cells were then treated with PBS containing 0.2% Triton-X 100 (Wako Pure Chemical

Industries, Ltd.) at room temperature for 15 minutes. After washing three times with PBS, cells were blocked for 20 minutes with 4% skim milk in PBS and then incubated with primary antibodies at 4°C overnight. The cells were washed three times with PBS, incubated with appropriate fluorescein-conjugated secondary antibodies and then counterstained with Hoechst33342 (Sigma-Aldrich Corporation, St. Louis, US). Primary and secondary antibodies used for immunocytochemical analysis are shown in Table S2.

PAS staining

PAS staining was performed according to the standard protocol using Cold Schiff's Reagent (Wako Pure Chemical Industries, Ltd.).

CYP3A4 activity

CYP3A4 activity was determined by CYP3A4 P450-Glo assay with Luciferin-IPA (Promega, Wisconsin, USA), according to the manufacturer's protocol.

ALB and urea assay

ALB and urea levels in the cell culture supernatant were determined by ALB ELISA kit or Urea Assay Kit (Abcam) according to the manufacturer's protocol.

Acetylated Low Density Lipoprotein (Dil-Ac-LDL) labeling

Cells were incubated with 5 μg/ml Dil-Ac-LDL (AlfaAesar, Massachusetts, US) for 4 hrs at 37^{o}C. Then cells were washed with PBS and counterstained with Hoechst33342.

Data analysis

Data are expressed as mean ± SEM and analyzed by Student's t-test. The statistical significance was determined at $P<0.05$.